Spectrochimica Acta Part A 83 (2011) 379–383

Contents lists available at SciVerse ScienceDirect

Spectrochimica Acta Part A: Molecular and Biomolecular Spectroscopy

journal homepage: www.elsevier.com/locate/saa

The synthesis and spectroscopic characterization of nano calcium fluorapatite using *tetra*-butylammonium fluoride

Mehdi Sheykhan[a], Akbar Heydari[a,*], Leila Ma'mani[b], Alireza Badiei[c]

[a] *Chemistry Department, Tarbiat Modares University, P.O. Box 14155-4838 Tehran, Iran*
[b] *Pharmaceutical Sciences Research Center, Tehran University of Medical Sciences, Tehran, Iran*
[c] *School of Chemistry, College of Science, University of Tehran, Tehran, Iran*

ARTICLE INFO

Article history:
Received 14 February 2011
Received in revised form 8 August 2011
Accepted 24 August 2011

Dedicated to memory of Davoud Karimi.

Keywords:
Bioactive material
Nano fluorapatite
Homogeneity
pH effects

ABSTRACT

Pure homogeneous nano sized biocompatible fluorapatite (FAp) particles were synthesized by a wet chemical procedure using water soluble *tetra*-butylammonium fluoride (TBAF) without using high temperatures and any purification processes. Combination of the Bragg's law and the plane-spacing equation for the two high intensity lines, namely, (0 0 2) and (3 0 0), gives $a = 9.3531$ Å, $c = 6.8841$ Å, confirms the identity of the highly crystalline synthetic material as well as its purity. The effect of various pH's in crystal formation and on their size was also evaluated. The calculated crystallinities were excellent with a rate around 5.0. The synthesized nano FAp was fully characterized by spectroscopic techniques (XRD, SEM, EDS, BET, FT-IR and ICP-AES). The nitrogen adsorption–desorption isotherm showed a type IV diagram and calculation of the surface area was investigated as well.

1. Introduction

Following its versatile applications in the field of bioceramics [1], drug delivery carriers [2,3], catalyst carriers [4], adsorbents [5] and acid base catalysis [6], interest has increasingly been drawn to calcium hydroxyapatite $Ca_{10}(PO_4)_6(OH)_2$ (HAp). In terms of catalysis, hydroxyapatite has been demonstrated to be proper of versatility in modification of surface, relative thermal and chemical stability and biocompatibility as one of the ideal materials for encapsulation of nanoparticles [7]. It has been well established that Ca^{+2} sites in HAp can be replaced by various transition metal cations, which have high catalytic activities [8]. However, poor corrosion resistance in acidic media [9], high dissolution rate under physiological conditions [10] and poor chemical stability at high temperatures [11] has restricted the application of calcium hydroxyapatite in catalysis. Among the apatite derivatives, fluorapatite (FAp), is considered as an alternative material due to its low solubility in organic solvents as well as in water, higher acid resistance than HAp [12], good biocompatibility [13] and high stability at high temperatures (the melting point of FAp is 1650 °C). Moreover, fluorine as a microelement is necessary for the normal dental and bone formation in the body [14]. Additionally, synthetic fluorapatite is an important material for the preparation of fluorescent lamps [15], laser host for neodymium [16] and praseodymium ions [17] and is used as humidity sensors [18]. The performance of FAp in all applications is influenced by its structural features such as size, morphology, crystallinity and purity. Therefore, it is of great importance that one is able to prepare FAp in nano size and controlled shape. There are several well-established records for the synthesis of FAp such as precipitation [19], hydrolysis [20], hydrothermal [21], glutamic acid [22], pH cycling [23], solid state reactions [24], using surfactants [25], biological proteins [26], chelating agents [27], hydrogen fluoride [28,29], sodium fluoride [29], ammonium fluoride [30–32], calcium fluoride in the presence of HAp followed by treatment with HNO_3 [33] and calcium fluoride [34]. However, the X-ray spectra of these methods show the formation of calcium oxide (CaO) [34], carbonate-hydroxyapatite, and low degree of crystallinities [29]. Also, there are some reports about formation of oxyapatite, resulting from degradation of contaminant hydroxyapatite in high temperatures [35]. In other words, methods using from high toxic row materials such as HF are not employed currently. Because of high thermal and mechanical stability in many cases removing of such phases is extremely difficult and will add time, cost and complexity to the overall process. Despite some of the above mentioned significant progresses, a facile synthesis not involving any template, specially leading to nano size particles remains a great challenge in this field. Because of the mentioned importance of the fluorine substituted apatites, this paper is concerned with the synthesis of fluorapatite nanoparticles through a wet chemical method using, water soluble *tetra*-butylammonium fluoride (TBAF) (Scheme 1). In addition to a structural study of the fluorapatite nanoparticles formed, the dependence on pH for

* Corresponding author. Tel.: +98 82883444; fax: +98 82883455.
E-mail address: akbar.heydari@gmx.de (A. Heydari).

1386-1425/$ – see front matter © 2011 Elsevier B.V. All rights reserved.
doi:10.1016/j.saa.2011.08.049

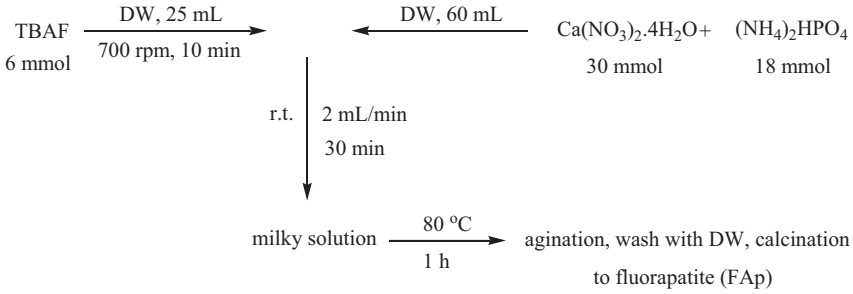

Scheme 1. Preparation of fluorapatite nanoparticles.

crystallinity, size and homogeneity and its spectroscopic properties were also studied.

2. Results and discussion

2.1. Scanning electron microscopy (SEM)

The statistical analysis (Fig. 1) for seventy-five observed particles confirms that the size distribution of nanoparticles is a narrow normal one with a 43.2 nm average value and a 2.2 nm standard deviation. Scanning electron micrograph (SEM) (Fig. 2a) clearly showed the synthetic material is present as uniform particles and of particle sizes less than 50 nm. The theoretical curve of standard distribution from these, was calculated by means of an excel program.

2.2. X-ray diffraction analysis (XRD)

The crystalline phase of FAp was found to be consistent with the literature values (JCPDS No. 15-0876). All the peaks in XRD pattern are in excellent agreement with the standard pattern and earlier studies for hexagonal crystal structure of fluorapatite [36]. The highest signal was found to be the (2 1 1), in agreement with that reported in the standard pattern. In this graph (Fig. 2b), signals at 10.8°, 22.0°, 25.9°, 28.1°, 29.1°, 32.2°, 33.2°, 34.1°, 40.0°, 42.2°, 46.8°, 48.3° and 49.6° are easily recognized from the XRD pattern. Signals at 10.8°, 22.0° and 33.2° are related to the (1 0 0), (2 0 0) and (3 0 0) reflections, respectively. While, the observed lines at 29.1° and 40.0° corresponded to other (*h k* 0) reflections, (2 1 0) and (3 1 0), respectively. The lines attributed to none (h k 0); (0 0 2), (1 0 2), (2 1 1), (2 0 2), (3 1 1), (2 2 2), (3 1 2) and (2 1 3) are those at 25.9°, 28.1°, 32.2°, 34.1°, 42.2°, 46.8°, 48.3° and 49.6°. Combination of the Bragg's law and the plane spacing equation gives Eq. (1), where $\lambda^2/4$ has a value of 0.595 Å^2 for Cu K_α radiation.

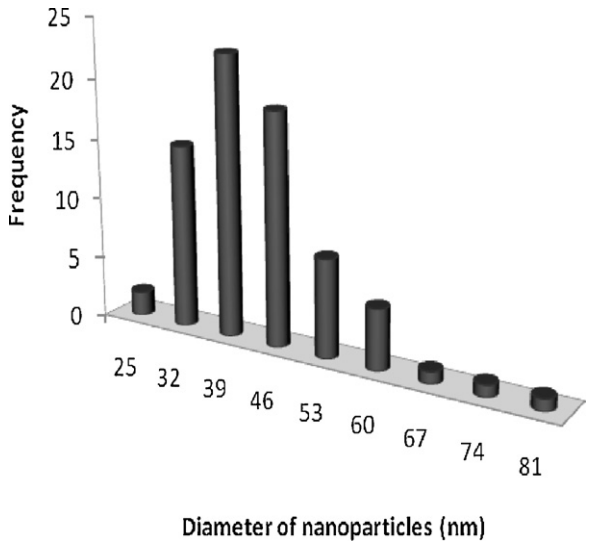

Fig. 1. The histogram of fluorapatite nanoparticles derived from the SEM image.

Lattice parameters calculation from XRD patterns:

$$\sin^2\theta = \frac{\lambda^2}{4}\left[\frac{4(k^2+kh+h^2)}{3a^2}+\frac{l^2}{c^2}\right] \quad (1)$$

Writing this equation out for the two high intensity lines, namely, (0 0 2) and (3 0 0), we obtain simultaneous solution of these two equations: It gives $a = 9.3531$ Å, $c = 6.8841$ Å (see Table 1 and Supplementary), which are closer to those reported in the literature [36]: $a = 9.3684$ Å and $c = 6.8841$ Å. These confirm that the synthetic material has high crystallinity as well as purity of the phase composition. Also, estimation of some parameters was done using PowderCell 2.4. The average unit cell parameters are about $a = 9.3672$ Å, $c = 6.8652$ Å and calculated data for 2θ are in close agreement with observed ones. Calculated amounts of 2θ and $\sin^2\theta$ inserted in Table 1 for comparison (see also Supplementary Fig. S4). Besides, no evidence of impurities such as calcium oxide and carbonate-hydroxyapatite can be found in the XRD patterns. The sharp and intense peaks indicate good crystallinity of the sample. According to the Debye–Scherrer equation, the calculated particle size of the FAp was 41.3 nm.

2.3. FT-IR spectrum of synthetic material

In FT-IR, the characteristic absorption bands due to vibration bending modes of O–P–O were observed in 595, 607 cm^{-1}. Also the stretching of the P–O bond appears at 1100 cm^{-1}. The OH's, immersed in an infinite chain of OH, produce a signal at 632 cm^{-1} in hydroxyapatite. Therefore the absence of medium signals at 632 and 867 cm^{-1} refute the presence of hydroxyapatite and HPO_4^{2-}, respectively. Additionally the absence of a sharp peak around 1410 cm^{-1} and a weak one at about 870 cm^{-1} can refute the presence of carbonate-hydroxyapatite (Fig. 2c).

2.4. Brunauer–Emmet–Teller surface analysis procedure

As we known the types of isotherms obtained for adsorption of gases on porous solids (type IV and type V) are different from those gained for adsorption on free surfaces. The differences resulted from the fact that the porous solid has an internal surface therefore the thickness of the adsorbed layers on the walls of the pores is limited by the width of the pores resulting in type IV and V isotherms, instead of type II and III ones. These isotherms are similar to type II, except that at high relative pressures the isotherm likes to reach a saturation value or increases asymptotically until it cuts the line at $p/p_o = 1$ at a small angle as compared to type II isotherms which approaches the line $p/p_o = 1$ quite asymptotically. In addition, these two isotherms often show a hysteresis loop, such that the amount of adsorbed at a given relative pressure is larger on the desorption